ARTICLE

# Temperature-Programmed Desorption Spectrometer Combining Minimum Gas Load, Fast Substrate Replacement, and Comprehensive Temperature Control

Shucai Xia[a,d], Shanshan Dong[a,d], Huizhi Xie[a,b], Jialong Li[a,c], Tianjun Wang[a], Weiqing Zhang[a], Li Che[c], Zefeng Ren[a], Dongxu Dai[a], Xueming Yang[a], Chuanyao Zhou[a,d*]

*a. State Key Laboratory of Molecular Reaction Dynamics, Dalian Institute of Chemical Physics, Chinese Academy of Sciences, Dalian 116023, China*
*b. Department of Chemical Physics, School of Chemistry and Materials Science, University of Science and Technology of China, Hefei 230026, China*
*c. Department of Physics, School of Science, Dalian Maritime University, Dalian 116026, China*
*d. University of Chinese Academy of Sciences, Beijing 100049, China*

(Dated: Received on December 26, 2022; Accepted on February 22, 2023)

With the capability of quantitative identifying surface species and measuring desorption kinetics, temperature-programmed desorption (TPD) is widely used in heterogeneous catalysis and surface science fields. Minimum gas load during adsorption, fast substrate replacement, and comprehensive temperature control are of great significance for efficient and high quality TPD experiments. Unfortunately, these requirements usually cannot be met at the same time for the existing apparatuses in surface science. In order to increase the universality, a TPD spectrometer combining minimum gas load, fast substrate replacement, and comprehensive temperature control in our laboratory has been built. By using an automatically controlled microcapillary array-based effusive molecular beam gas doser, optimizing the thermal contact at the sample stage, using liquid nitrogen transfer line and designing thermocouple connection, controllable and reproducible molecule adsorption, minimum gas load, fast substrate replacement, rapid cooling, accurate temperature measuring and excellent linear heating are achieved simultaneously. Capabilities of the TPD spectrometer, for example, determination of desorption energy and desorption order, quantitative measurements of surface species and binding sites, and investigation of surface photochemical reactions, are demonstrated by measuring the desorption of water from highly oriented pyrolytic graphite and $TiO_2(110)$ and photocatalyzed oxidation of methoxy anions on $TiO_2(110)$. The apparatus described here will contribute effectively to the high throughput measurements.

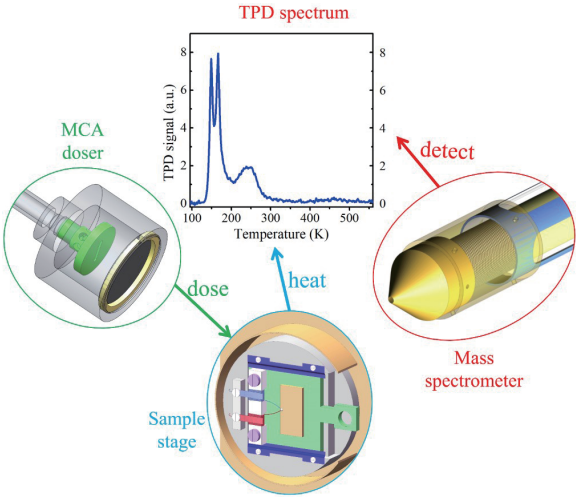


**Key words:** Temperature-programmed desorption, Fast substrate replacement, Thermal desorption spectroscopy

* Author to whom correspondence should be addressed. E-mail: chuanyaozhou@dicp.ac.cn

 

## I. INTRODUCTION

Molecule-surface interactions play a key role in many processes including gas sensing, thin film growth, adsorptive separation of gas mixture and especially heterogeneous catalysis [1–4]. Investigating the adsorption and reaction of molecules on surfaces, such as, binding sites, adsorption state (molecular or dissociative) and possible reaction products, is therefore of great significance to understand their interactions. Scanning tunneling microscopy (STM) is a powerful technique to image the adsorption on surfaces at the atomic level [5]. However, its poor chemical identification capability and its requirement of conductive substrates substantially limit the application of STM in tracing surface species. Infrared spectroscopy (IR) and temperature-programmed desorption (TPD) are widely used in heterogeneous catalysis and surface science to study the adsorption and quantitatively measure the chemical species at surfaces [6, 7]. Different from metal materials, the absence of image dipoles on dielectric substrates makes the application of reflective infrared absorption spectroscopy (IRAS) to bulk dielectric materials very difficult [8]. In contrast, TPD measures the desorbing chemical species by mass spectroscopy (MS), thus is not sensitive to substrates from the technical point of view.

The basic principle of TPD is to detect the partial pressure of desorbing species from substrates which are linearly heated as a function of substrate temperature. The mass to charge ratio ($m/z$), desorbing temperature, intensity and profile in TPD spectra convey the information of chemical species, binding sites (binding energy), coverages and desorption order, respectively [9, 10]. The desorption rate of molecules from substrate surfaces can be described by Polanyi–Wigner equation [9, 11].

$$-\frac{\mathrm{d}\theta}{\mathrm{d}t} = -\frac{\mathrm{d}\theta}{\mathrm{d}T}\cdot\beta = \upsilon\cdot\theta^n\cdot\exp\left(-\frac{E_{\mathrm{des}}}{RT}\right) \qquad (1)$$

Where $\theta$, $t$, $T$, $\beta$, $\upsilon$, $n$, $E_{\mathrm{des}}$, and $R$ stand for the coverage, time, substrate temperature, linear heating rate, pre-exponential factor, desorption order, desorption energy, and gas constant, respectively.

In TPD measurements, the signal of desorbing species ($I$) detected by the mass spectrometer is proportional to the desorption rate. By taking the natural logarithm of both sides, Eq.(1) can be converted to Eq.(2).

$$\begin{aligned}\ln I \propto \ln\left(-\frac{\mathrm{d}\theta}{\mathrm{d}t}\right) &= \ln\left(-\frac{\mathrm{d}\theta}{\mathrm{d}T}\right) + \ln\beta \\ &= \ln\left(\upsilon\cdot\theta^n\right) - \frac{E_{\mathrm{des}}}{RT}\end{aligned} \qquad (2)$$

If $E_{\mathrm{des}}$ and $\upsilon$ are independent of the temperature and coverage, the first term on the right side of Eq.(2) is constant. Therefore, the desorption energy can be calculated from the slope ($-E_{\mathrm{des}}/R$) obtained by a linear fitting of the Arrhenius plot ($\ln I$ versus $1/T$) without prior knowledge of desorption order. At the leading edge of TPD spectra, molecules have just started to desorb and the coverage change is small, so both the coverage and desorption energy can be regarded as coverage independence [12]. Then $E_{\mathrm{des}}$ values at different coverages can be obtained by fitting the Arrhenius plots at the leading edges. However, TPD signal at the leading edge is usually weak, which might lead to large data fitting errors. Therefore, high-quality experimental data are needed for the application of the leading edge analysis (LEA) method.

A typical TPD spectrometer mainly consists of three parts [13, 14], namely gas dosing, temperature control, and mass spectrometer detection. The function of a gas doser is to deliver target molecules onto the substrate surface. An ideal gas doser should prepare a uniform molecule-substrate interface with desired coverage and minimum gas load. Temperature control is critical to the quality of the TPD spectra. Ideally, accurate temperature measuring, rapid substrate cooling, and stable linear heating are needed. However, for TPD spectrometers in surface science, back filling adsorption is the first choice [15, 16], which leads to serious gas load problem. Fast substrate replacement is needed for high throughput measurements. Unfortunately, fast substrate replacement and comprehensive temperature control usually can not be satisfied simultaneously. To the best of our knowledge, there is no existing TPD spectrometer in surface science field which combines the minimum gas load, fast substrate replacement, and comprehensive temperature control.

Back filling adsorption through leak valve causes severe gas load problem, especially for those species difficult to pump (for example, water). In addition, back filling leads to adsorption everywhere in the chamber, resulting in interference of desorption from areas in the proximity of the target substrate. Although single pinhole directional gas dosers can limit the exposure area of gases, they will prepare inhomogeneous coverages

DOI: 10.1063/1674-0068/cjcp2212180 

across the substrate surfaces [17]. By using microcapillary arrays (MCA), effusive molecular beam dosers can deliver molecules to substrate surface with significantly improved homogeneity over the single pinhole doser and has much less gas load and higher efficiency [14, 17–20].

Precise control of the target molecule coverage is important to investigate the adsorption behavior. In surface chemistry, the coverage (1 L=$1\times10^{-6}$ torr·s) is usually referred to as the product of target gas pressure in the ultrahigh vacuum (UHV) chamber and the exposure time. For a manually controlled leak valve, it is extremely difficult to keep the gas pressure constant during the whole exposure period. Although this problem can be solved by using an automatic pneumatic valve [15], it still leads to heavy gas load. The gas doser is usually equipped with a gas handling system (GHS) [14, 21], which is used to purify the liquid/gaseous samples and prepare some vapor in the gas storage for subsequent adsorption. The dosing amount is adjusted by controlling the dosing time at a pre-set gas pressure in the gas storage. To achieve an accurate and reproducible dosing, especially for the preparation of surfaces with small coverages, automatic dosing is highly desired.

Temperature control is critical to the quality of the TPD spectra. Accurate temperature measuring is the premise to get an accurate desorption energy. Rapid cooling on one hand can efficiently reduce the adsorption of residual gas such as water in the UHV chamber, minimizing the effect of co-adsorption from undesired molecules. This point is getting more important if the adsorption of desired molecule is weaker than the residual gas in the chamber. For example, $H_2O$ preferentially binds to $TiO_2$(110) over $CO_2$ due to the adsorption energy difference [22]. On the other hand, gas dosing is usually performed at low substrate temperature, then fast cooling can significantly improve the efficiency of experiments if one needs to repeat the cooling-adsorption-TPD cycles. Linear heating is a widely used heating mode in TPD experiments due to its experimental convenience and ease of analyzing desorption kinetics. An excellent heating performance is the prerequisite to obtain accurate desorption kinetic parameters.

The quality of temperature control is associated with the style of substrate installation. In surface science field, substrates are either fixed at the end of the manipulator or can be transferred together with the sample plate between the vacuum chambers. Fast substrate replacement and comprehensive temperature control are of great significance for efficient and high quality TPD experiments. However, these two requirements usually cannot be met at the same time. For a fixed substrate style, comprehensive temperature control can be achieved but the chamber needs to be ventilated for substrate replacing, which prevents the high throughput measurements. If the substrate can be transferred, the temperature control is a big problem. First, the substrate transferability is usually achieved at the cost of thermal contact, leading to slower cooling. Typically, it takes more than an hour for the transferrable substrate to cool from 800 K to 120 K. Second, the thermocouple wires are usually spot welded or fixed at the clamps which are pressed against the sample plate for convenience rather than directly on the substrate surface in the transferrable style (FIG. 4), resulting in deviation between the measured temperature and the actual value at the substrate surface. In the TPD experiments, the sample should be heated at a constant rate of 2 K/s, which means the thermal equilibrium between the substrate and the clamp may not be established during the ramp. And the temperature difference between the substrate and the sample stage will change rather than keep constant during the heating process.

For most of the existing TPD spectrometers in surface science field, substrates are fixed at the sample stage [16, 23–27]. Haegel *et al.* presented an improved sample stage that can fix three samples and heat them separately [15]. However, the flexibility is still limited. Hanna *et al.* reported a TPD spectrometer that allowed fast substrate replacing, but the temperature control needed to be improved [28]. While Stuckenholz *et al.* proposed a TPD setup for portable substrates, complicated mechanical work was involved in the transfer in UHV and a leak valve doser was used [29]. Magerl *et al.* proposed an attosecond photoelectron spectroscopy setup that enabled fast sample replacement and precise temperature control, and an MCA doser was used, but in this work the TPD experiments were performed using a modified Bayard-Alpert pressure gauge, and no details about the structure and design of the TPD spectrometer were shown [30].

In order to increase the universality, a TPD spectrometer combining minimum gas load, fast substrate replacement and comprehensive temperature control has been built in our laboratory. By using an automati-

DOI: 10.1063/1674-0068/cjcp2212180 

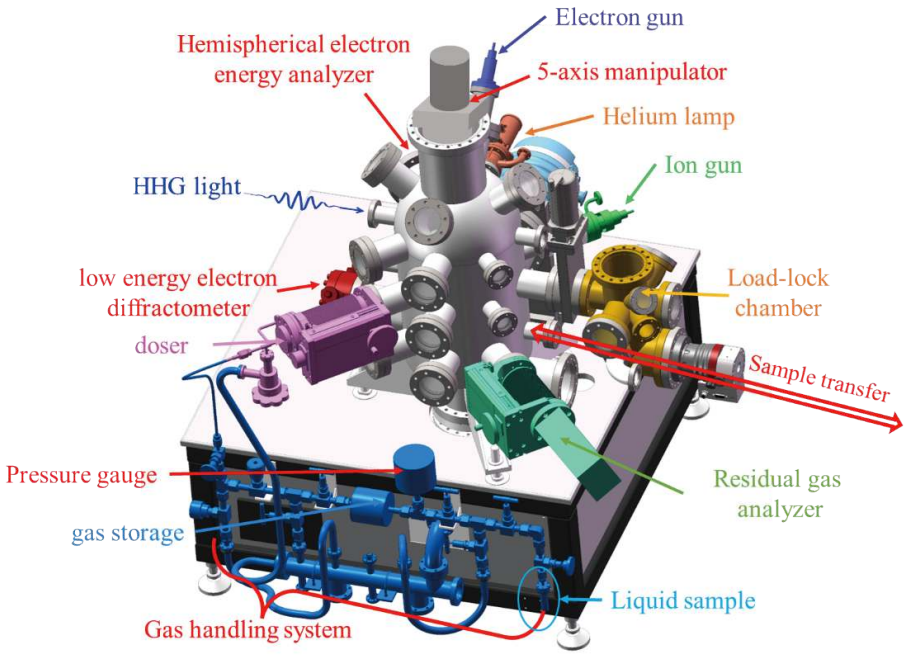


FIG. 1 Three-dimensional design of the UHV system. Devices and sub-systems are shown in different colors.

cally controlled MCA-base effusive molecular beam doser, optimizing the thermal contact at the sample stage, using liquid nitrogen transfer line, and designing thermocouple connection; controllable and reproducible molecule adsorption, minimum gas load, fast substrate replacement, rapid cooling, accurate temperature measuring and excellent linear heating are achieved simultaneously. The capabilities of the TPD spectrometer are demonstrated by measuring the desorption of water from highly oriented pyrolytic graphite (HOPG) and $TiO_2$(110) and photocatalyzed oxidation of methoxy anions on $TiO_2$(110).

## II. EXPERIMENTAL SETUP

### A. The UHV system

The UHV system (Prevac) consists of a loadlock chamber and a main chamber (FIG. 1). The loadlock chamber, which is pumped by a 70 L/s turbo molecular pump and a 2 L/s dry pump to allow the storage of six substrates under a vacuum of better than $1\times10^{-8}$ mbar, is attached to the main chamber via a gate valve for fast sample loading and transferring. A TPD and an angle-resolved photoelectron spectrometer (ARPES) are integrated in the main chamber. The main chamber is made of μ-metal to shield the geomagnetic field, which is essential for ARPES measurements. An ultrahigh vacuum better than $2\times10^{-10}$ mbar is achieved by using the combination of a 700 L/s turbo molecular pump, a 2 L/s dry pump, and a titanium sublimation pump. The main chamber is equipped with preparation and characterization devices. An argon ion gun (IQE 11/35; SPEC), a low energy electron diffractometer (LEED 600; OCI Vacuum), and an electron gun (QE 10/35; SPECS) are installed for crystal substrate cleaning, LEED, and Auger electron spectroscopy (AES) characterization, respectively. The substrate is located at the bottom of a five-axis manipulator (Prevac), which enables the transfer along $X$, $Y$, and $Z$ and the rotation around $Z(\theta)$ and the substrate normal ($\varphi$).

### B. The TPD spectrometer

#### 1. The gas dosing part

The gas dosing part is composed of a GHS and an MCA doser. Details of the GHS are schematically shown in FIG. 2. The GHS can be divided into the liquid/gaseous sample purification, the gas storage, and the exposure time control parts. The GHS is constructed by stainless steel tubes and valves, which is pumped through a common tube by a 70 L/s turbo molecular pump and a 2 L/s dry pump. All the tubes can be baked by heating tapes, and a base vacuum of better than $2\times10^{-8}$ mbar can be achieved, which reduces the contamination of gases in GHS entering the UHV chamber.

Purification of the liquid/gaseous sample is needed

DOI: 10.1063/1674-0068/cjcp2212180 

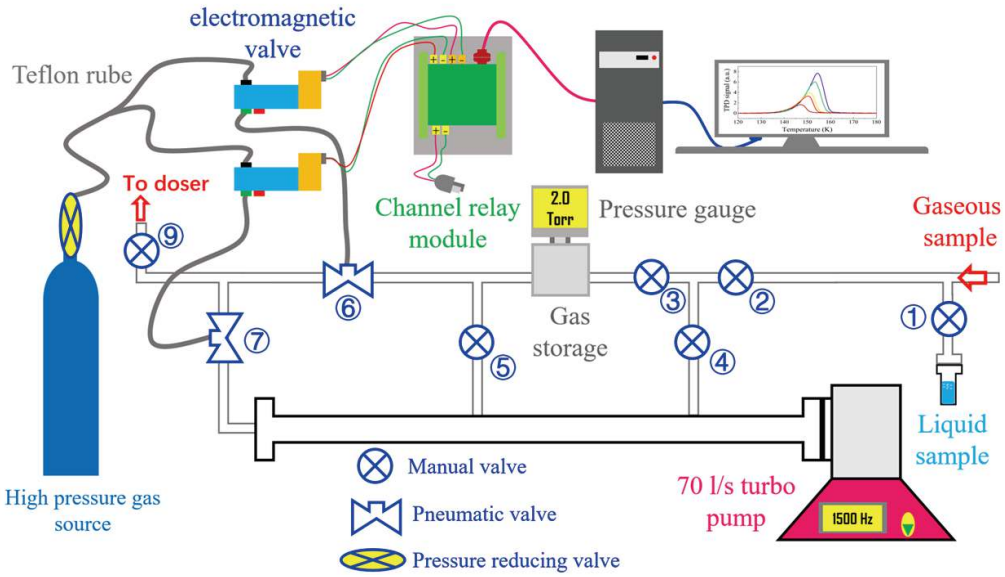


FIG. 2 Schematic of the gas handling system (GHS).

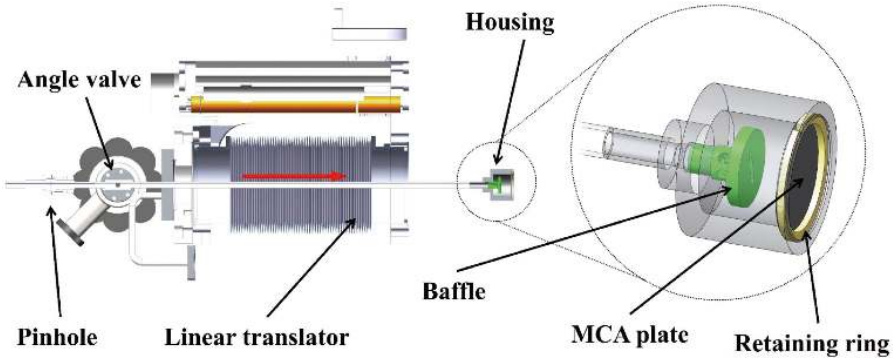


FIG. 3 Detailed structure of the microcapillary arrays (MCA) molecular beam doser mounted in a linear translator, and the enlarged view of the head of doser is also shown.

before adsorption. Liquid sample is stored in a small stainless steel tank that is connected to the GHS via valve 1. Through freeze-pump-thaw method, air in the tank can be pumped out and the liquid sample is purified. For the gaseous sample, the tubes connecting the GHS are baked and pumped after every ventilation. According to the gas species, a trap using liquid nitrogen/dry ice/water-ice mixture is used to freeze possible impurities.

A 0.4 L gas storage is used to store the sample vapor with a desired pressure for the subsequent adsorption. The gas pressure is monitored by a gauge (0.1–760 torr) and adjusted by using the manual valves (valve 1, valve 2 and valve 3) between the sample tank and the gas storage. If the gas pressure is higher than the target value, the excess gas can be evacuated by opening valve 5. Valves 6 and 7 are pneumatic (PM) valves that are normally closed and can be opened when the pressure of driving gas ($N_2$) exceeds 5 bar. When valve 6 is open and valve 7 is closed, gases diffuse from the gas storage to the gas doser. When the adsorption is finished, gases between valve 6 and the gas doser can be pumped away immediately through valve 7. In order to automatically control the dosing duration, high pressure gas driving the pneumatic valves are regulated by two electromagnetic (EM) valves whose working statuses are manipulated by a computer-controlled channel relay. In this way, the accuracy of gas exposure time can reach 0.2 s.

FIG. 3 shows the schematic of the gas doser which is mounted on a linear translator to adjust its distance from the substrate surface. First, the vapor flux from the gas storage is reduced by a 7-micronmeter pinhole which is drilled at the center of a VCR gasket [31]. The molecular beam then spreads from left to right in a 1/4-inch stainless steel tube as indicated by the red arrow. When the molecular beam arrives at the housing, it is blocked by a baffle, and flows out through six holes drilled on the side of it [18]. Finally, the molecular beam

DOI: 10.1063/1674-0068/cjcp2212180 

passes through the MCA plate (plate diameter: 13 mm; thickness: 1 mm; channel diameter: 7 μm; distance between channels: 10 μm; bias angle: 0 degree), and is uniformly exposed to the substrate surface. To minimize the dead space, a retaining ring is used to fix the MCA plate resulting in an effective diameter of 11 mm, which is slightly larger than the typical substrate size of 5 mm×8 mm. For an efficient preparation of uniform adsorbates, the size of the MCA plate in the doser should be slightly larger than that of the substrate and the distance from the substrate should be small enough [17, 19, 20]. Therefore, during dosing, the doser-to-substrate distance is kept as small as possible, and a typical value of 2 mm can be reached, which is much smaller than those around 25 mm reported previously [27, 29, 32]. As the exposure area is more localized, the signal from areas outside the substrate is significantly suppressed in the TPD measurements. In a typical dosing of water onto the 100 K $TiO_2$(110) (a pressure of 2 torr in the gas storage), the water partial pressure in the main chamber measured by the mass spectrometer (the ion source is about 30 cm away from the doser head) increases from $2\times10^{-10}$ mbar to $6\times10^{-10}$ mbar, and it takes only a few tens of seconds to prepare 1 ML water on the substrate. To get a similar coverage by the back filling method under this pressure, it takes over 30 min to get a assuming sticking coefficient of 1. The quantitative comparison clearly shows the high efficiency and low gas load in the adsorption with the MCA doser. More important, dosing through a microcapillary array can substantially improve the uniformity of the adsorbates [17, 19, 20], which is crucial to analyze and interpret the experimental data. In addition, there are some experiments that require successive adsorption of different gases to the substrate. After the dosing of the first gas, it is necessary to quickly remove the remaining gas in the gas dosing system for subsequent dosing. However, the pump speed in the region between pinhole and MCA plate is slow, so an angle valve is installed here and connected to the pumping line for efficient gas exchange.

### 2. The temperature control part

Temperature control is realized by electron bombardment heating and liquid nitrogen cooling, which are integrated inside the sample stage at the bottom end of the manipulator, allowing the substrate temperature to be manipulated between 90 K and 1273 K. Liquid nitrogen is led to a reservoir close to the sample stage by a transfer line (ST400; Janis) from a self-pressurized dewar. FIG. 4(a) shows the schematic of the bottom end of the 5-axis manipulator with a substrate inserted. The N type thermocouple (ULTRA-TEMP 516; AREMCO) is glued directly onto the substrate surface (for example, $TiO_2$) for accurate temperature reading, and the other ends of two thermocouple wires are wrapped around a ceramic strip which is fixed at the left side of the widely used flag style sample plate. To avoid electrical contact between thermocouple wires and the sample plate, two grooves are machined on the bottom side of ceramic strip. The substrate is installed onto the tantalum sample plate, which can be easily inserted into or pulled out from the sample stage by using the mechanical arm as long as the sample stage is moved to the calibrated position and angle, and it takes no more than 5 min to complete the whole substrate replacing process. The contact between the thermocouple wires and thermocouple connectors can be optimized by changing the turns of thermocouple wires wound on ceramic strip, so the temperature reading can remain stable for each substrate. The transfer in the current work seems simpler than that reported in a TPD setup for portable substrates [29]. When the sample plate is inserted, the thermocouple wires on its left side contact the thermocouple connectors at the sample stage, so that the substrate temperature is measured. FIG. 4(b) shows the temperature curve for two consecutive heating-cooling cycles. Owing to the fast liquid nitrogen transferring and firm contact of the components at the sample stage, it takes less than 15 min to cool the substrate from 800 K to 100 K, which is much shorter than the typical value of 1 h in surface chemistry apparatuses, thus minimizing residual gas adsorption and increasing the efficiency of experiments. In our design, both the thermocouple connectors and the clamps compress the substrate against the sample stage, which provides stable thermal connection between them. After more than 400 heating-cooling cycles and 50 substrate replacements over 6 months, the drop in cooling rate does not exceed 10%.

At a heating rate of 2 K/s, a linear fit of the temperature data points from 120 K to 800 K yields a correlation coefficient of 0.999, suggesting an excellent linear heating. Moreover, the performance at a lower heating rate of 1 K/s is as perfect as that at 2 K/s. Too slow heating requires fairly accurate measurements, and too

DOI: 10.1063/1674-0068/cjcp2212180 

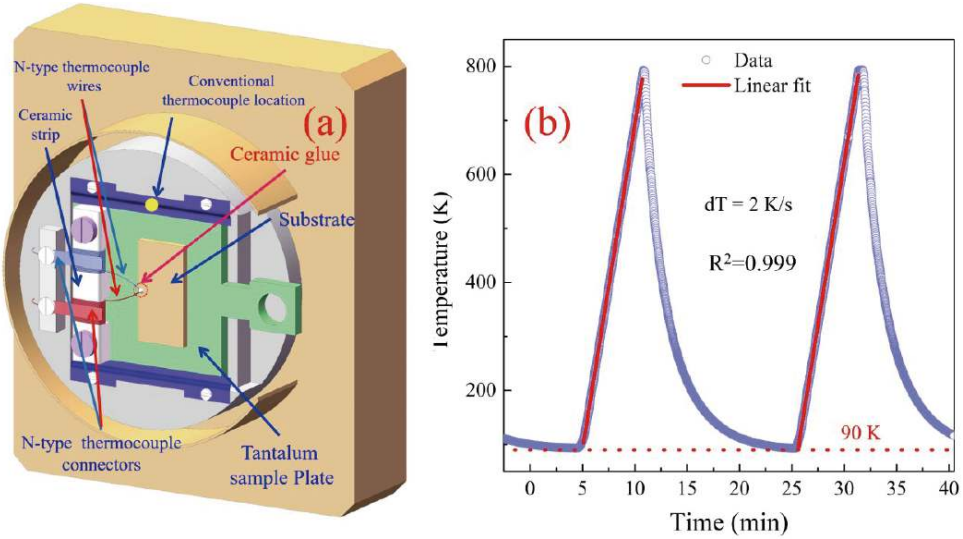


FIG. 4 (a) Schematic of the sample stage located at the bottom of manipulator with a sample plate inserted. (b) Temperature curve for two consecutive heating-cooling cycles.

fast heating requires adequate pumping speed. Therefore, in our experiments, we selected the moderate heating rate of 1 K/s or 2 K/s.

#### 3. The mass spectrometer detection part

Desorbing species from the substrate are detected by a shielded quadrupole mass spectrometer (QMS; RGA 200; SRS), which is also a residual gas analyzer (FIG. 5). The ion source of the QMS is shielded by a cylindrical copper shell, which is mounted on the stainless steel shield support on one side and connected with a copper skimmer with a 2 mm aperture on the other side. Large holes are machined on the side wall of the shield support to achieve sufficient pumping speed. Mounted on a linear translator, the skimmer-to-substrate distance can be easily adjusted, and is kept at approximately 0.2 mm during TPD measurements, which is closer than those in previous studies (typically 0.5–3 mm) [29, 32–34]. However, such small distance makes the intensity of TPD signal more sensitive to the distance [35]. In order to ensure a constant distance for different TPD measurements, an aluminum block is mounted on the linear translator. When the linear translator moves and contacts with the Al block, its position is fixed, and then the skimmer-to-substrate distance can be precisely adjusted by using the micrometer on the manipulator. This small distance and the small skimmer aperture (compared to a typical substrate size of 5 mm) make the sampling of desorbed species almost exclusively from the substrate surface. Both the PID temperature control unit and the mass spectrometer are remotely-controlled by a self-written LabView program, allowing the automatic TPD data acquisition.

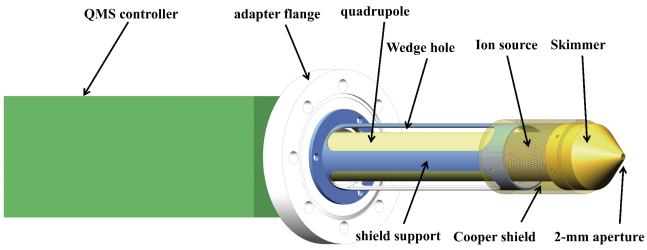


FIG. 5 Schematic of the shielded QMS, the stainless steel shield support, cooper shield and skimmer are connected in turn.

## III. EXPERIMENTAL RESULTS

Water desorption from HOPG and rutile $TiO_2(110)$ and photocatalyzed oxidation of methoxy anions on $TiO_2(110)$ were measured to test the performance of the TPD spectrometer.

### A. Water desoption

#### 1. Water desorption from highly oriented pyrolytic graphite

Water desorption from HOPG was measured to analyze the desorption order and desorption energy. HOPG substrate was cleaved using tape in air and annealed in UHV at 1000 K for several hours. Since the connection between the glue and the HOPG substrate is relatively weak, a thermocouple was spot welded to a location near the substrate on the tantalum sample plate. Water coverages on HOPG were varied by changing the

DOI: 10.1063/1674-0068/cjcp2212180 

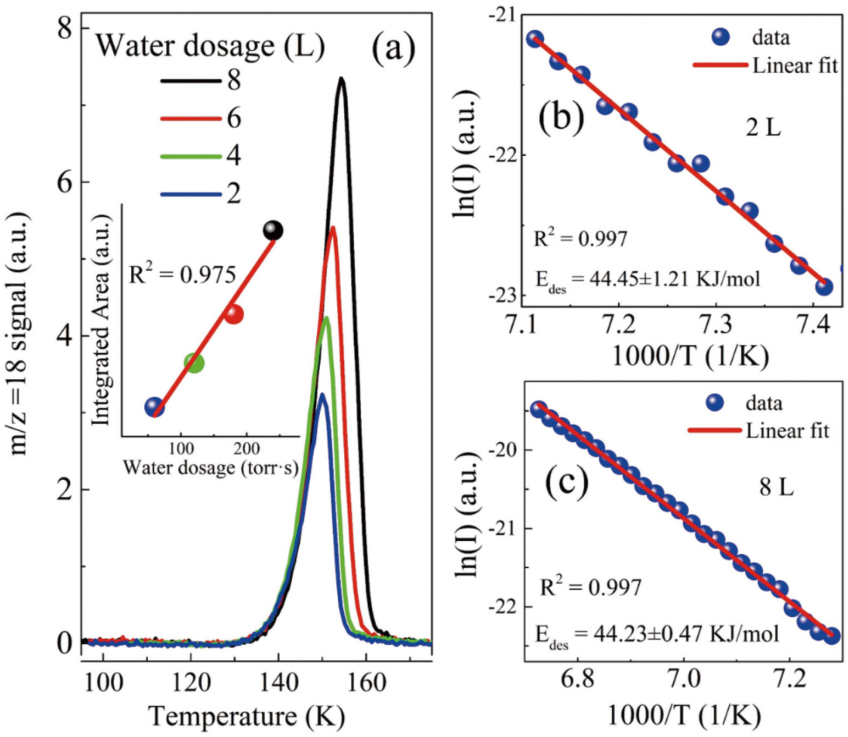


FIG. 6 (a) Water TPD spectra from HOPG. Inset of (a) shows the integrated area of spectra as a function of water dosage and a linear fit. (b) and (c) are the Arrhenius plot based on the leading edge of TPD spectra with water dosage of 2 L and 8 L. Linear fittings of the two plots yield desorption energies of 44.45±1.21 kJ/mol and 44.23±0.47 kJ/mol, respectively.

water exposure time at a vapor pressure of 3 torr and a substrate temperature of 115 K. Corresponding water ($m/z$=18) TPD spectra collected at a heating rate of 1 K/s are shown in FIG. 6(a). Leading edges of the spectra are well aligned above 145 K but have a little deviation at lower temperature range, indicating imperfect zero-order desorption kinetics [36].

In the current experiments, the absolute coverage of water on HOPG is difficult to determine, but it can be represented by the integrated area under each spectrum. The inset of FIG. 6(a) shows the integrated area of the TPD spectra as a function of water dosage. The data points can be well fitted by a straight line, suggesting a constant sticking coefficient under the current experimental conditions, which is consistent with previous studies [36, 37].

Averaged from three sets of data, TPD spectra in FIG. 6(a) are smooth enough and LEA method was applied to calculate the desorption energy of water on HOPG. Then LEA analysis was performed in the region of leading edge where the initial desorption was within 5% of the original coverage for each spectrum. FIG. 6 (b) and (c) show two Arrhenius plots based on the leading edges of TPD spectra with water dosage of 2 L and 8 L. Both data sets can be perfectly fitted by a straight line, from which the desorption energies are calculated to be 44.45±1.21 kJ/mol and 44.23±0.47 kJ/mol, respectively. Using the same method, desorption energies of 44.86±0.8 KJ/mol and 46.13±1.14 kJ/mol are obtained for the other two spectra with water dosage of 4 L and 6 L. The desorption energy values in this work agree well with previous ones [36, 37]. Furthermore, the desorption energies for different coverages are very close, suggesting their coverage independence [36].

### 2. Water desorption from rutile $TiO_2$(110)

Desorption of water from $TiO_2$(110) was measured to test the capability of the TPD spectrometer to identify binding sites. The $TiO_2$ sample was prepared with conventional cycles of $Ar^+$ sputtering (1 keV) and UHV annealing (900 K) until a sharp LEED pattern can be seen and no contamination can be detected by AES. After that, we found the outgassing of the ceramic glue is very small and is absolutely negligible as long as the aperture of the skimmer on QMS is not facing to the glue. HPLC grade water (Sigma-Aldrich) was purified through cycles of freeze-pump-thaw with the gas han-

DOI: 10.1063/1674-0068/cjcp2212180 

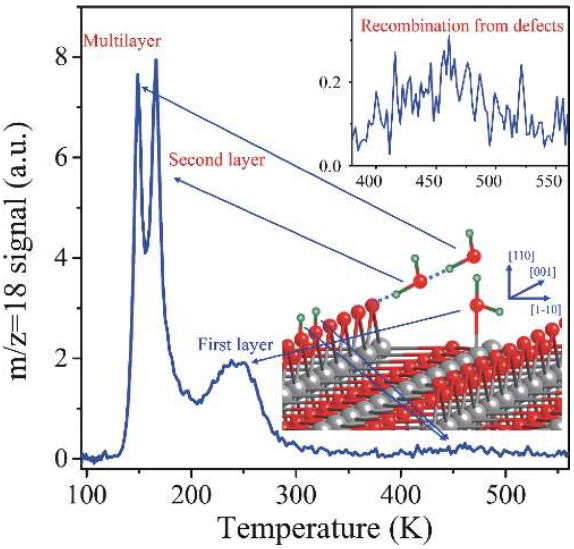


FIG. 7 TPD spectrum of 2.8 ML water on rutile $TiO_2$(110) collected with a heating rate of 2 K/s. The upper inset shows the enlarged zone around 460 K, and the lower inset is the ball and stick model of rutile $TiO_2$(110) substrate with water molecules adsorbed at different sites.

dling system. TPD experiments were carried out with a heating rate of 2 K/s. The desorption spectrum of 2.8 monolayer (ML, 1 ML corresponds to the density of fivefold coordinated Ti ions ($Ti_{5c}$) on the (110) surface of rutile $TiO_2$, *i.e.*, $5.2\times10^{14}$ $cm^{-2}$) $H_2O$ ($m/z$=18) from $TiO_2$(110) is shown in FIG. 7. Four desorption features centered at 149 K, 167 K, 250 K and 460 K are detected, which are assigned to desorption of multilayer, the second layer (binding to bridging oxygen), the first layer (binding to $Ti_{5c}$ on the surface) water and recombination of bridging hydroxyls (formed by spontaneous dissociation of water at the bridging oxygen vacancies) according to a previous study [38]. By comparing the signal of the recombination and the first layer desorption feature, the density of bridging oxygen vacancies can be calculated to be about 4%.

### B. Photocatalyzed oxidation of methoxy anions on rutile $TiO_2$(110)

Photocatalyzed oxidation of methoxy anions on $TiO_2$(110) was measured to analyze reaction products. The preparation and desorption of methoxy groups on $TiO_2$(110) have been well documented [39, 40]. By co-adsorbing oxygen with methanol, $CH_3OH$ molecules adsorbed at fivefold coordinated Ti sites can react with the O atoms generated by the dissociation of $O_2$ on the surface to produce methoxy anions (Reaction (1)).

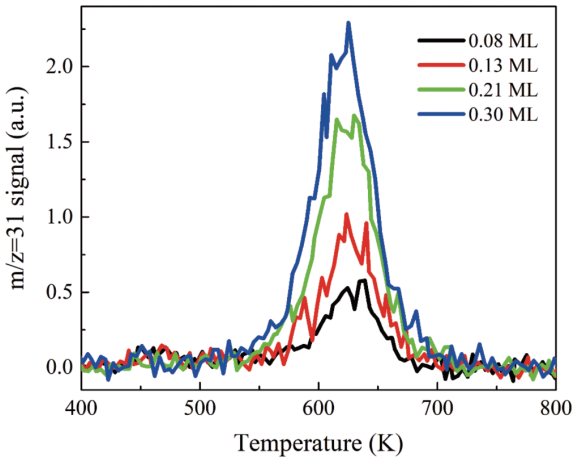


FIG. 8 TPD spectra of methanol ($m/z$=31) from $TiO_2$(110) as a function of methoxy anion coverage. The spectra are collected with a heating rate of 2 K/s.

$$CH_3OH_{Ti_{5c}} + O_b{}^{2-} \rightarrow CH_3O_{Ti_{5c}}{}^{-} + O_bH^{-} \text{ (at 90 K)} \quad \text{(R1)}$$

where subscript "$Ti_{5c}$" and "b" represent the species absorbed at fivefold coordinated Ti sites and bridging sites, respectively. The quantity of methoxy anions produced is dependent of the available charge at the surface and subsurface region of $TiO_2$. As the $TiO_2$ substrate in the current work is only slightly reduced, the available charge is limited, which further limits the coverage of methoxy anions to 0.30 ML. Varying the coverage of methoxy anions within 0.30 ML requires precise control of gas dosing which can be realized by our computer-controlled gas dosing system. Having been exposed to 40 torr·s $O_2$ (99.9999%, Arkonic), the 90 K $TiO_2$(110) surface was further exposed to purified $CH_3OH$ (HPLC grade, Sigma-Aldrich) ranging from 20 torr·s to 100 torr·s. After that, the $TiO_2$ substrate was flashed to 450 K to remove residual oxygen and methanol, leaving a methoxy anions covered surface.

The coverage of methoxy anions on $TiO_2$(110) was measured by TPD. Upon heating, $Ti_{5c}$ bounded methoxy anions experience disproportionation reaction to produce methanol and formaldehyde around 640 K (Reaction (2)) [40].

$$2CH_3O_{Ti_{5c}}{}^{-} \rightarrow CH_2O_{(g)} + CH_3OH_{(g)} \text{ (at 640 K)} \quad \text{(R2)}$$

where (g) represents the gaseous species, TPD spectra of methanol ($m/z$=31) from $TiO_2$(110) surfaces are shown in FIG. 8 as a function of methoxy anion coverage. By comparing with the TPD spectra of the saturated first methanol layer on $TiO_2$(110) (0.77 ML with re-

DOI: 10.1063/1674-0068/cjcp2212180 

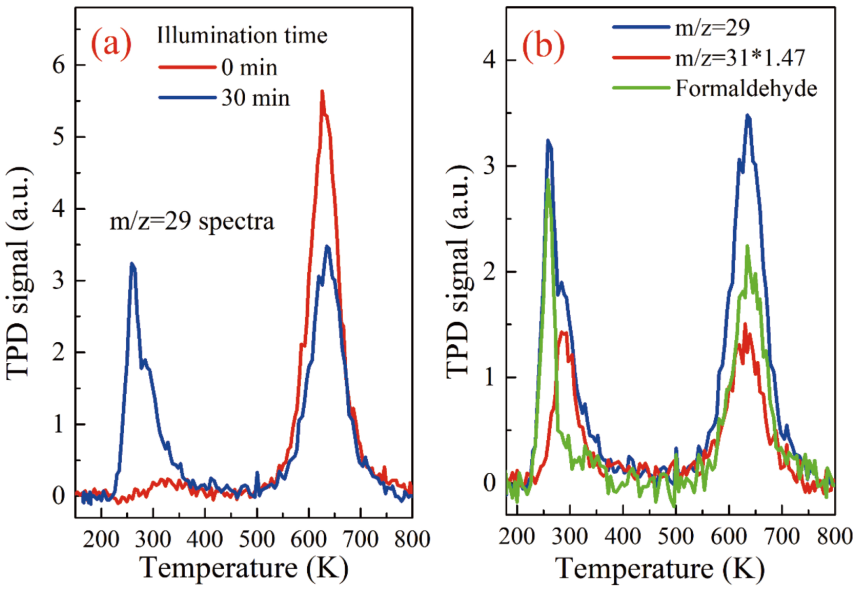


FIG. 9 (a) TPD spectra ($m/z$=29) of 0.3 ML methoxy anions covered $TiO_2$(110) surface before and after 405 nm light illumination, respectively. (b) By subtracting the contribution from methanol of the TPD spectrum, the $m/z$=29 signal of formaldehyde is obtained.

spect to the density of $Ti_{5c}$ [41]), the absolute coverages of methoxy anions are calculated to be 0.08, 0.13, 0.21 and 0.30 ML. According to the spectral line shape and the shift of the peak position with increasing coverage, the desorption of methoxy anions from $TiO_2$(110) obeys the second-order kinetics [42], which is consistent with the disproportionation reaction (Reaction (2)).

Following the preparation, photocatalyzed oxidation of methoxy anions on $TiO_2$(110) was measured. The photochemical reaction was initiated by 405 nm light, and more experimental details can be found in our previous work [43]. FIG. 9(a) shows TPD spectra ($m/z$=29) from 0.30 ML methoxy anions covered $TiO_2$(110) as a function of light illumination. Exposed to light for 30 min, the signal at 640 K is reduced by 38.7 %, and two peaks at 270 K and 320 K appear. Photochemistry of methoxy anions on $TiO_2$(110) involves the production of methanol and formaldehyde. While the fragmentation of both $CH_3OH$ and $CH_2O$ contribute to the TPD spectra of $m/z$=29, that of $m/z$=31 comes solely from $CH_3OH$. For the mass spectrometer used in the current work, the ratio of the detection efficiency of $m/z$=29 to $m/z$=31 is 1.47 for methanol. By subtracting the contribution of $CH_3OH$ ($1.47\times(m/z=31)$ signal) to $m/z$=29 signal (green line in FIG. 9(b)), a single peak at 270 K shows up. Drawing analogy to the desorption of formaldehyde from $TiO_2$(110) [39, 43–45], the signal of $m/z$=29 at 270 K is attributed to the desorption of $CH_2O$ which is generated from the photocatalyzed oxidation of methoxy anions on $TiO_2$(110) (Reaction (3)).

$$CH_3O_{Ti_{5c}}{}^{-} + O_b{}^{2-} + h\nu \rightarrow CH_2O_{Ti_{5c}} + O_bH^{-} \quad \text{(R3)}$$

## IV. CONCLUSION

In summary, a universal TPD spectrometer combining minimum gas load, fast substrate replacement, and comprehensive temperature control has been built in our laboratory. An automatically controlled microcapillary array-based effusive molecular beam doser is used, which improves the homogeneity, increases the reproducibility, and minimizes the gas load. By optimizing the thermal contact at the sample stage, using liquid nitrogen transfer line and designing thermocouple connection, fast substrate replacement, rapid cooling, accurate temperature measuring, and excellent linear heating are achieved simultaneously. The capabilities of this TPD spectrometer have been demonstrated by several desorption experiments.

## V. ACKNOWLEDGEMENTS

This work was supported by the National Key Research and Development Program of China (No.2021YFA1500601 and No.2018YFA0208703), the National Natural Science Foundation of China (No.21973010 and No.21973092), the Instrument Developing Project of the Chinese Academy of Sciences

DOI: 10.1063/1674-0068/cjcp2212180 

(No.YZ201504), the CAS Projects for Young Scientists in Basic Research (No.YSBR-007), the Dalian Institute of Chemical Physics Innovation Foundation (DICP I202205), and LiaoNing Revitalization Talents Program (No.XLYC1907032).

[1] T. Seiyama, A. Kato, K. Fujiishi, and M. Nagatani, Anal. Chem. **34**, 1502 (1962).
[2] W. Stephen, Adv. Mater. **27**, 5720 (2015).
[3] J. R. Li, R. J. Kuppler, and H. C. Zhou, Chem. Soc. Rev. **38**, 1477 (2009).
[4] J. M. Herrmann, Catal. Today **53**, 115 (1999).
[5] B. C. Stipe, M. A. Rezaei, and W. Ho, Science **280**, 1732 (1998).
[6] A. Yee, S. J. Morrison, and H. Idriss, J. Catal. **186**, 279 (1999).
[7] Q. Guo, C. Zhou, Z. Ma, Z. Ren, H. Fan, and X. Yang, Chem. Soc. Rev. **45**, 3701 (2016).
[8] Y. Wang, A. Glenz, M. Muhler, and C. Woell, Rev. Sci. Instrum. **80**, 113108 (2009).
[9] D. A. King, Surf. Sci. **47**, 384 (1975).
[10] P. A. Redhead, Vacuum **12**, 203 (1962).
[11] C. T. Campbell and J. R. V. Sellers, Chem. Rev. **113**, 4106 (2013).
[12] E. Habenschaden and J. Kuppers, Surf. Sci. **138**, L147 (1984).
[13] S. M. Gates, J. N. Russell, and J. T. Yates, Surf. Sci. **159**, 233 (1985).
[14] J. T. Yates Jr., *Experimental Innovations in Surface Science*, *1st Edn.*, New York: Springer, (1998).
[15] S. Haegel, T. Zecho, and S. Wehner, Rev. Sci. Instrum. **81**, 033904 (2010).
[16] S. Bag, R. G. Bhuin, R. R. J. Methikkalam, T. Pradeep, L. Kephart, J. Walker, K. Kuchta, D. Martin, and J. Wei, Rev. Sci. Instrum. **85**, 014103 (2014).
[17] J. M. Guevremont, S. Sheldon, and F. Zaera, Rev. Sci. Instrum. **71**, 3869 (2000).
[18] G. L. Fisher and C. A. Meserole, J. Vac. Sci. Technol. A **23**, 722 (2005).
[19] C. T. Campbell and S. M. Valone, J. Vac. Sci. Technol. A **3**, 408 (1985).
[20] D. E. Kuhl and R. G. Tobin, Rev. Sci. Instrum. **66**, 3016 (1995).
[21] M. J. Bozack, L. Muehlhoff, J. N. Russell Jr., W. J. Choyke, and J. T. Yates Jr., J. Vac. Sci. Technol. A **5**, 1 (1987).
[22] R. S. Smith, Z. Li, L. Chen, Z. Dohnalek, and B. D. Kay, J. Phys. Chem. B **118**, 8054 (2014).
[23] C. Kim, X. M. Yan, and J. M. White, Rev. Sci. Instrum. **71**, 3502 (2000).
[24] Z. F. Ren, Q. Guo, C. B. Xu, W. S. Yang, C. L. Xiao, D. X. Dai, and X. M. Yang, Chin. J. Chem. Phys. **25**, 507 (2012).
[25] B. R. Chalamala, D. Uebelhoer, and R. H. Reuss, Rev. Sci. Instrum. **71**, 320 (2000).
[26] A. V. Matveev, E. M. Sadovskaya, A. A. Bryliakova, and V. V. Gorodetskii, J. Mol. Catal. A Chem. **420**, 18 (2016).
[27] E. T. Jensen, Phys. Chem. Chem. Phys. **23**, 3748 (2021).
[28] T. Hanna, H. Hiramatsu, I. Sakaguchi, and H. Hosono, Rev. Sci. Instrum. **88**, 053103 (2017).
[29] S. Stuckenholz, C. Büchner, H. Ronneburg, G. Thielsch, M. Heyde, and H. J. Freund, Rev. Sci. Instrum. **87**, 045103 (2016).
[30] E. Magerl, S. Neppl, A. L. Cavalieri, E. M. Bothschafter, M. Stanislawski, T. Uphues, M. Hofstetter, U. Kleineberg, J. V. Barth, D. Menzel, F. Krausz, R. Ernstorfer, R. Kienberger, and P. Feulner, Rev. Sci. Instrum. **82**, 063104 (2011).
[31] P. L. Hagans, B. M. DeKoven, and J. L. Womack, J. Vac. Sci. Technol. A **7**, 3375 (1989).
[32] M. Accolla, E. Congiu, F. Dulieu, G. Manicò, H. Chaabouni, E. Matar, H. Mokrane, J. L. Lemaire, and V. Pirronello, Phys. Chem. Chem. Phys. **13**, 8037 (2011).
[33] P. Feulner and D. Menzel, J. Vac. Sci. Technol. **17**, 662 (1980).
[34] J. Lallo, E. V. Lee, R. Lefkowitz, and B. J. Hinch, Surf. Sci. **606**, 320 (2012).
[35] H. Schlichting and D. Menzel, Surf. Sci. **285**, 209 (1993).
[36] A. S. Bolina, A. J. Wolff, and W. A. Brown, J. Phys. Chem. B **109**, 16836 (2005).
[37] D. V. Chakarov, L. Osterlund, and B. Kasemo, Vacuum **46**, 1109 (1995).
[38] M. A. Henderson, Surf. Sci. **355**, 151 (1996).
[39] M. Shen and M. A. Henderson, J. Phys. Chem. Lett. **2**, 2707 (2011).
[40] M. A. Henderson, S. Otero-Tapia, and M. E. Castro, Faraday Discuss. **114**, 313 (1999).
[41] Z. Li, R. S. Smith, B. D. Kay, and Z. Dohnálek, J. Phys. Chem. C **115**, 22534 (2011).
[42] Y. Lilach, I. M. Danziger, and M. Asscher, Catal. Lett. **76**, 35 (2001).
[43] S. Dong, J. Hu, S. Xia, B. Wang, Z. Wang, T. Wang, W. Chen, Z. Ren, H. Fan, D. Dai, J. Cheng, X. Yang, and C. Zhou, ACS Catal. **11**, 2620 (2021).
[44] Q. Guo, C. Xu, Z. Ren, W. Yang, Z. Ma, D. Dai, H. Fan, T. K. Minton, and X. Yang, J. Am. Chem. Soc. **134**, 13366 (2012).
[45] C. Xu, W. Yang, Q. Guo, D. Dai, T. K. Minton, and X. Yang, J. Phys. Chem. Lett. **4**, 2668 (2013).

DOI: 10.1063/1674-0068/cjcp2212180 